Published in final edited form as:
Cancer Res. 2011 June 15; 71(12): 4074–4084. doi:10.1158/0008-5472.CAN-10-3968.

mTOR kinase inhibitor AZD8055 enhances the immunotherapeutic activity of an agonist CD40 antibody in cancer treatment

Qun Jiang[1], **Jonathan M. Weiss**[1], **Timothy Back**[1], **Tim Chan**[1], **John R. Ortaldo**[1], **Sylvie Guichard**[2], and **Robert H. Wiltrout**[1]

[1]Laboratory of Experimental Immunology, CIP, CCR, NCI-Frederick, Maryland [2]AstraZeneca, Macclesfield, UK

Abstract

Mammalian target of rapamycin (mTOR) is a central mediator of cancer cell growth, but it also directs immune cell differentiation and function. On this basis, we have explored the hypothesis that mTOR inhibition can enhance cancer immunotherapy. Here we report that a combination of αCD40 agonistic antibody and the ATP-competitive mTOR kinase inhibitory drug AZD8055 elicited synergistic anti-tumor responses in a model of metastatic renal cell carcinoma. In contrast to the well-established mTOR inhibitor rapamycin, AZD8055 increased the infiltration, activation and proliferation of CD8+ T cells and NK cells in liver metastatic foci when combined with the CD40 agonist. AZD8055/ αCD40-treated mice also display an increased incidence of matured macrophages and dendritic cells compared to that achieved in mice by αCD40 or AZD8055 treatment alone. We found that the combination treatment also increased macrophage production of TNFα; which played an indispensable role in activation of the observed anti-tumor immune response. Levels of Th1 cytokines, including IL-12, IFN-γ, TNFα, and the Th1-associated chemokines RANTES, MIG and IP-10 were each elevated significantly in the livers of mice treated with the combinatorial therapy versus individual treatments. Notably, the AZD8055/ αCD40-induced anti-tumor response was abolished in IFN-γ −/− and CD40 −/− mice, establishing the reliance of the combination therapy on host IFN-γ and CD40 expression. Our findings offer a preclinical proof of concept that, unlike rapamycin, the ATP-competitive mTOR kinase inhibitor AZD8055 can contribute with αCD40 treatment to trigger a restructuring of the tumor immune microenvironment to trigger regressions of an established metastatic cancer.

Keywords

mTOR; CD40; macrophage; IFN-γ; CD8 T cells

Introduction

The mammalian Target of Rapamycin (mTOR) plays a central role in regulation of cell growth and proliferation by monitoring nutrient availability, cellular energy levels, oxygen levels and mitogenic signals (1). It exists in two distinct complexes — mTOR Complex 1 (mTORC1) and mTOR Complex 2 (mTORC2). mTORC1 is characterized by the classic features of mTOR as a nutrient/energy/redox sensor and regulator of protein synthesis (1);

Disclosure of Potential Conflicts of Interest
The authors report no potential conflicts of interest.

mTORC2 has been shown to function as an important regulator of the actin cytoskeleton and Akt activation (2, 3). The mTOR pathway is dysregulated in many kinds of human diseases, especially certain cancers, which suggests it could be a good target for cancer therapy (4, 5). Rapamycin and its pharmacologic analogs (e.g. sirolimus and RAD001) are preferentially effective at blocking mTORC1, which could also have the unwanted side-effect of disengaging the mTORC1 negative feedback loop, thereby causing PI3K-AKT over-activation and impairment of overall anti-tumor efficacy (6). Therefore, ATP-competitive inhibitors of mTOR kinase, which target both mTORC1 and mTORC2 (7) and more profoundly inhibit of 4E-BP1 phosphorylation by mTORC1 (8, 9), are anticipated to have broader application and perhaps increased activity when used in combination with other anti-tumor agents.

Besides direct effects on tumor cells, studies in the past few years have reported a broad spectrum of regulatory effects on both innate and adaptive immune cells by mTOR inhibition (10). Rapamycin exerts its potent immunosuppressive effects through restricting proliferation of T cells and NK cells (11, 12), and inhibiting differentiation, maturation and function of innate immune cells *in vitro*, including DCs and macrophages (13–15). These types of effects could be presumed to impair anti-tumor immune responses. However, rapamycin-mediated inhibition of mTOR can also cause an increase in the production of pro-inflammatory cytokines, such as IL-12, IL-23 and IL-6 by innate immune cells, and can also decrease the production of the anti-inflammatory cytokine IL-10 following LPS stimulation. Moreover, even though rapamycin can act directly on T cells to suppress their proliferation and effector function, it also has been shown to increase the ability of LPS-stimulated monocytes to prime Th1 cells *in vitro* (16). Finally, rapamycin-induced autophagy has been reported to increase antigen presentation in DCs *in vivo*(17). These immune modulating effects of mTOR inhibition suggest mTOR-inhibiting drugs could synergize with more traditional immune modulators for induction of anti-tumor responses.

CD40 is a TNF receptor family member that plays a critical role in both humoral and cellular immune responses (18). It has a broad pattern of expression, including APCs, B cells, endothelial cells, as well as some tumor cells (18). Agonistic αCD40 antibodies, a potent mimic of the natural ligand CD154, have been shown to promote T cell-mediated immunity in treatment of cancers in experimental animal models through activation of APCs (19, 20). In some tumor models, the effector cells were shown to be $CD8^+$ T-cells and macrophages, and it has been reported that a stimulatory αCD40 antibody indirectly activated NK cells by IL-12 secreted by $CD40^+$ DCs and monocytes, which resulted in significant antitumor activity (21). The successes achieved with agonistic αCD40 mAbs in preclinical models has led to clinical evaluation of anti–human CD40 mAbs as a potential treatment for cancer (22, 23).

In this study, we hypothesized that combining the ATP-competitive inhibitor, AZD8055, with αCD40 antibody would induce more efficient anti-tumor effects by a combination of direct tumor killing and subsequent release of tumor associated antigens to antigen-presenting cells, and co-incident modulation of immune cell functions in vivo. The results of our study demonstrate, in a syngeneic mouse metastatic RCC model, that AZD8055 and αCD40 synergize for tumor regression by activating macrophages and DCs and inducing strong Th1 immune responses in the tumor microenvironment.

Materials and Methods

Reagents

AZD8055 was supplied by AstraZeneca (Macclesfield, UK). Rapamycin was purchased from LC Labs (Woburn, MA, USA). For *in vitro* studies, AZD8055 was prepared as a 10

mmol/l stock solution in DMSO. For studies in mice, AZD8055 and rapamycin were prepared in sterile water with 0.5% HPMC, 0.1%polysorbate 80 and one-third of overall final volume of glass beads, and then shaken overnight to generate an homogenous suspension. Agonist rat anti-mouse CD40 (clone FGK115B3) was purified from ascites, as previously described (24). Endotoxin was <1 EU/mg antibody, as determined by chromogenic Limulus Amebocyte Lysate kit (Cambrex). Purified rat IgG was purchased from Jackson ImmunoResearch Laboratories. Monoclonal antibodies obtained from BD PharMingen (Chicago, IL) included anti-mouse CD3ε (clone 145-2C11, clone 500A2), anti-mouse CD8 (clone 53-6.7), anti-mouse CD86 (clone GL-1), anti-mouse MHC Class II (I-A/I-E) (clone M5/114.15.2), anti-mouse CD69 (clone H1.2F3), anti-mouse IL-12 (p40/p70) (clone C15.6). Monoclonal antibodies obtained from eBiosciences (San Diego, CA) included anti-mouse F4/80 (clone BM8), anti-mouse NKp46 (clone 29A1.4), anti-mouse CD11c (clone N418), NKG2D (clone CX5), anti-mouse IFN-γ (clone XMG1.2), anti-mouse TNFα (clone MP6-XT22). Pacific orange-conjugated rat anti-mouse CD45 (clone 30-F11) was purchased from Invitrogen (San Diego, CA).

Mice and tumor cells

BALB/c wild-type mice were obtained from the Animal Production Area of the National Cancer Institute-Frederick Cancer Research and Development Center (Frederick, MD). BALB/c IFN-γ KO (GKO) mice were obtained from the Jackson Laboratories (Bar Harbor, ME), and then bred at NCI-Frederick. Mutant alleles were confirmed by PCR genotyping. All mice were maintained in a dedicated pathogen-free environment and used between 7 and 10 weeks of age in accordance with an approved NCI Frederick Institutional Animal Care and Use protocol. For tumor cell lines used in this study, Renca (murine renal carcinoma) was obtained from Dr. Pontes (25); the streptozotocin-induced RCC cell line was developed by our lab (26); and the B16-F10 mouse melanoma was obtained from Dr. Josh Fidler (1982). All cell lines were tested using the molecular testing of biological materials assay for murine cells in 2007. Tumor cell lines were maintained in RPMI 1640 medium with 10% FBS (FBS), 2 mM L-glutamine, 1×nonessential amino acids, and 1 mM sodium pyruvate. For studies in mice, Renca tumors were maintained by serial i.p. passage in syngeneic mice. eGFP-Renca was prepared by transducing Renca cells with lentiviral pLenti6/EF1a/eGFP expression vector in the presence of 5μg/ml polybrene (Sigma), which was created using Gateway Technology (Invitrogen) by site-specific recombination between pDEST/eGFP, pDEST-5'-EFIα promoter and pLenti6/R4R2/V5—DEST vectors. RENCA/eGFP clones were selected by adding 5μg/ml blasticidin to the RPMI media and then confirming > 90% eGFP expression by flow cytometry.

Liver tumor model

Renca cells were injected intrasplenically at a dose of 0.4×10^5 cells (Renca) or 2×10^5 (GFP-Renca) on day 0, and splenectomies were done on all mice immediately after tumor injection. Mice were then treated with vehicle control for AZD8055 (0.5% HPMC, 0.1%polysorbate 80, oral gavage) and IgG control for CD40 antibody (i.p.), CD40 antibody (65 μg, i.p.), AZD8055 (20mg/kg weight, oral gavage) or rapamycin (2mg/kg weight, oral gavage), according to the schedules outlined for each experiment. All mice were then euthanized on day 17; livers were harvested into Bouin's Solution; and the number of tumor nodules was counted using a dissecting microscope.

Histology Assay

Livers were dissected, and fixed in 10% neutral buffered formalin and then embedded in paraffin. Sections were cut at 5μm in thickness, deparaffinized in xylene, and serially dehydrated in decreasing concentrations of ethanol. Sections were stained with hematoxylin-

eosin and examined under light microscopy to detect lymphocyte infiltration and evaluate tissue structure.

Cell depletion *in vivo*

$CD8^+$ T cells were depleted *in vivo* using i.p. injections of rat anti-mouse CD8 (clone 19–178), starting on day 2 and continuing 3 times weekly (≥90% depletion). Control mice received 10% normal rat serum. To deplete NK cells, mice were given rabbit anti-asialo-GM1 i.v. (Wako Chemicals, Richmond, VA) on days 2, 4, 6, 9, 13 after tumor cell implantation in the liver (≥90% depletion). Control mice received 10% normal rabbit serum. For macrophage depletion, mice were injected i.v. with 100 μl of clodronate-liposomes on days -1, 2, 6, 10, 14 after tumor cell implantation into the liver (≥90% depletion). Clodronate-liposomes were obtained from Dr. N. van Rooijen (Vrije Universiteit, Amsterdam, Netherlands). PBS-containing liposomes were used as a control.

Isolation of liver leukocytes

On day 14 or 17, mice were euthanized and the livers flushed with 10 mL of HBSS through the portal vein, removed, homogenized using a GentleMACS™ Dissociator (Miltenyi Biotec, Gladbach, Germany), and then digested in RPMI containing 5% FCS, 250 U/mL type IV collagenase (Invitrogen), 100 μg/mL DNase I (Roche Molecular Biochemicals) and 1 mM EDTA (pH 8.0), at 37 °C for 20 min. The homogenate was then processed in a tissue stomacher-80 (Seward) for 30s, washed with HBSS (BioWhittaker), and resuspended in 40% Percoll (Amersham Pharmacia) in DMEM (BioWhittaker). The suspension was underlaid with 80% Percoll and centrifuged for 25 min at 1,000×g. Leukocytes were collected from the interphase, filtered with a 70μm Nylon cell strainer (BD Biosciences), washed, and enumerated on a Sysmex KX-21 (Roche, Indianapolis, IN) automated cell counter.

Flow cytometric analysis

Flow cytometric analysis was performed on liver leukocytes according to a previously described procedure (27). Briefly, cells (1×10^6) were incubated in cell staining buffer (0.1% BSA, 0.1% sodium azide) containing 250μg/mL 2.4G2 ascites for 25 min. Cells were stained with diluted fluorescently-conjugated antibodies for 30 min followed by two washes in staining buffer. Labeled cells were analyzed on an LSR-II flow cytometer (Becton Dickinson). For Ki67 staining, FITC-mouse anti-human Ki67 set (BD PharMingen) was used according to the manufacturer's suggested protocol. For IFN-γ intracellular staining, hepatic mononuclear cells (MNCs) were restimulated with PMA (5ng/ml)/Ionomycin (1μg/ml) for 4 h and 1μg/ml brefeldin A (GolgiPlug™) for another 5 h at 37°C in 5% CO2. For the detection for TNFα and IL-12, the restimulation conditions were 3 h-LPS (100 ng/ml) plus 5 h- Brefeldin A, and 2 h-LPS (1μg/ml) plus 10 h- Brefeldin A, respectively. After surface protein staining, cells were fixed using the Cytofix/Cytoperm kit (PharMingen), and then stained with optimally titered anti-mouse IFN-γ, TNFα, and IL-12.

Quantitative real-time PCR analysis

Livers obtained on day 17 were placed in RNALater (Ambion). Total RNA was isolated from liver homogenates using TRIzol (Invitrogen), precipitated, and then reverse transcribed (Applied Biosystems, Foster City, CA). RT2 real-time SYBR Green/Rox PCR master mix and RT2 Profiler PCR array were used for murine cytokines and chemokines detection (SuperArray). Genes of interest were subsequently examined with greater sensitivity by real time RT-PCR using TaqMan® Universal PCR Master Mix and the ABI Prism 7300 Detection System (TaqMan; Applied Biosystems) according to the manufacturer’s instructions. Primer sets for mouse included IL-12(p35) (Mm00434169), TNFα

(Mm00443258), IFN-γ (Mm99999071), CCL5 (Mm01302428), CXCL10 (Mm00445235), and CXCL9 (Mm00434946) (Applied Biosystems). Gene expression was normalized to the level of the β-actin housekeeping gene. Data were analyzed using the ΔΔCT method (28) and expressed as a fold change in mRNA expression relative to control values.

Statistical analysis

P values were determined by unpaired student's t test. $P < 0.05$ was considered statistically significant.

Results

AZD8055, but not rapamycin, induces enhanced antitumor immune responses in vivo when combined with αCD40

Based on reports that AZD8055 induces a profound growth inhibition, autophagy and cell death in many human tumor cell lines (29, 30) and our previous study showing that Renca tumor cells express functional CD40 (24), we first tested the direct effect of AZD8055 and αCD40 on the survival of Renca tumor cells *in vitro*. We found that only AZD8055 inhibited Renca cell growth, while αCD40 could neither inhibit Renca growth directly nor enhance the inhibitory ability of AZD8055 (Fig. 1A). To evaluate the anti-tumor effect *in vivo*, we designed and evaluated a variety of different schedules for the administration of AZD8055 in combination with αCD40 (Fig. 1B), in an experimental Renca liver metastasis model. The results showed that priming the immune system with αCD40 prior to the use of AZD8055 which directly targets the tumor cells (Fig. 1B schedule *a*) was the most active approach among the schedules utilized (Fig. 1C). These findings suggest administration of AZD8055 before or at the same time αCD40 delivery might suppress some immune functions and thereby impair the immune-priming function of subsequently delivered αCD40. Therefore, schedule *a* (αCD40 prior to AZD8055) which yielded the best overall anti-tumor effect was used in all subsequent studies, although significant tumor reduction was also observed with each of the other schedules tested.

In contrast to the anti-tumor effects of AZD8055 and αCD40 alone, we found that AZD8055/ αCD40 combination treatment induced a substantial reduction in both number (Fig. 2A) and size (data not shown) of tumor nodules in liver, although both agents administered alone also had some anti-tumor effects. The enhanced anti-tumor efficacy of the combination was also demonstrated in a Renca orthotopic model where Renca cells were injected under the kidney capsule and allowed to metastasize spontaneously (Supplementary Fig. S1). We also observed that the anti-tumor responses achieved by AZD8055/αCD40 were largely abrogated in CD40 −/− mice bearing Renca (Supplementary Fig. S2), which indicates that host CD40 expression is necessary for the anti-tumor response in *vivo*. We also hypothesized that a major contribution of mTOR inhibitor-induced tumor apoptosis would be the liberation of tumor antigen from killed cells, which could further promote maturation and T cell-priming function of antigen-presenting cells in response to αCD40. Therefore, we expected similar enhanced anti-tumor effects to be achieved when αCD40 was combined with different mTOR inhibitors. However, when αCD40 was combined with the classical mTOR inhibitor rapamycin, the anti-tumor responses achieved by the combination were indistinguishable from those achieved by rapamycin alone (Fig. 2A). Importantly, we observed a remarkable infiltration of $CD8^+$ T cells, DCs and macrophages into the livers of AZD8055/αCD40-treated mice, but not in the group treated with rapamycin/αCD40 (Fig. 2B), when compared to either vehicle control or αCD40 alone treated groups. These results demonstrated that the AZD8055 ATP-competitive mTOR kinase inhibitor, but not rapamycin, induced enhanced anti-tumor activities when combined

with αCD40, suggesting substantially different mechanisms of action on the immune system for AZD8055, compared to rapamycin.

We also investigated the anti-tumor effects of AZD8055/αCD40 in several other tumor models. Using the streptozotocin-induced, CD40 positive, RCC cell line that we characterized previously (26), we observed that AZD8055/αCD40 exhibited enhanced anti-tumor efficacy *in vivo* that was comparable to that observed for Renca (Supplementary Fig. S3A). We also used the CD40 negative B16 melanoma cell line in order to potentially address whether tumor-associated CD40 expression might contribute to the αCD40-mediated immune or anti-tumor effects. In contrast to the two RCC models previously described, neither AZD8055 nor αCD40, or the combination of AZD8055/αCD40, had any appreciable ability to reduce the number of B16 tumor nodules in the liver (Supplementary Fig. S3B). It is noteworthy, however, that regardless of the tumor model, the AZD8055/αCD40 combination still elicited significant immune cell infiltration *in vivo*. Taken together, it appears that RCC, may be particularly amenable to the AZD8055/αCD40 combination therapy.

AZD8055/αCD40 induces activation and proliferation of $CD8^+$ T cells and NK cells

To further delineate the immune effects induced by AZD8055 and αCD40, we examined the livers of treated mice and found that although αCD40 alone induced some recruitment of immune cells to the liver, αCD40 plus AZD8055 induced amore pronounced lymphocytic infiltration. In addition, there was a pronounced localization of leukocytes around tumor foci in response to αCD40/AZD8055 while few leukocytes were found in or around tumor foci in the vehicle control and AZD8055-treated groups (Fig. 3A). To determine the activation of $CD8^+$ T cells and NK cells, hepatic mononuclear cells (MNCs) of tumor-bearing mice were isolated on day 14 and subjected to flow cytometric analysis. AZD8055 plus αCD40 induced a significant elevation in the expression of CD69 and NKG2D on $CD8^+$ T cells (Fig. 3B). Among NK cells, $CD69^+$ and $NKGD2^+$ cell frequencies were also moderately increased in the combination-treated group (Fig. 3B). Furthermore, there was a notable up-regulation of Ki67 protein in both NK cells and $CD8^+$ T cells from AZD8055/αCD40-treated mice (Fig. 3C), suggesting that the expansion of these cell types might be at least partially due to proliferation. Moreover, we also found significant induction of IFN-γ expression in $CD8^+$ T cells and NK cells derived from AZD8055/αCD40-treated mice (Fig. 3D).

AZD8055/αCD40 matures and activates macrophages and DCs

Since AZD8055 could significantly increase the frequency of macrophages and DCs in liver when combined with αCD40 (Fig. 2B), we next investigated the effect of AZD8055/αCD40 on the status of antigen-presenting DCs and macrophages *in vivo*. Using eGFP-expressing Renca cells, we detected increased efficiency of processing of tumor-derived antigen by macrophages and DCs in AZD8055/αCD40-treated mice (Fig. 4A). Additionally, the maturation markers CD86 and MHC II were significantly up-regulated on macrophages and DCs (Fig. 4B). Increased production of IL-12 was also observed in macrophages and DCs from the AZD8055-alone group and in macrophages from the combination group (Fig. 4C). In addition, TNFα production was only significantly induced in macrophages by AZD8055/αCD40 treatment (Fig. 4D). Overall, these results demonstrated that macrophages and DCs were matured and activated in the AZD8055/αCD40-treated group.

$CD8^+$ T cells, NK cells and Macrophages all contribute to AZD8055/αCD40-induced anti-tumor responses

We next used antibodies to deplete $CD8^+$ T cells and NK cells before AZD8055/αCD40 treatment and found that depletion of either cell type could partially mitigate the anti-tumor response. The depletion of both cell types could substantially reduce the anti-tumor response

to the level achieved with AZD8055 alone (Fig. 5A), suggesting that CD8+ T cells and NK cells might contribute to the enhanced anti-tumor effect induced by the combination treatment. Furthermore, using macrophage depletion, we demonstrated a dramatic loss of anti-tumor activity by AZD8055/αCD40 thereby confirming a unique and indispensable role of macrophages in the anti-tumor immune responses induced by AZD8055/αCD40 combination treatment (Fig. 5B).

Anti-tumor immune responses induced by AZD8055/αCD40 depend on Th1 cytokines

Since we observed a significant degree of infiltration and activation of immune cells in the AZD8055/αCD40-treated tumor bearing mice, we hypothesized that this process would be associated with increased levels of cytokines and chemokines induced by AZD8055/αCD40. Therefore, we analyzed liver tissue from treated mice for gene expression by qPCR. AZD8055/αCD40 treatment significantly increased Th1 cytokines and Th1-associated chemokine expression in the liver, including IL-12, IFN-γ, TNFα, CCL5/RANTES, CXCL10/IP-10 and CXCL9/MIG (Fig. 6A), while αCD40 alone only slightly induced IL-12, CCL5, CXCL9 production, as compared to AZD8055 alone and vehicle control groups. Due to the high levels of IFN-γ production and previous studies showing the role of IFN-γ in this Renca model (31), we evaluated its role in the in vivo therapy. As shown in Figure 6B, AZD8055/αCD40-mediated anti-tumor responses were completely abolished in IFN-γ KO mice as was as the activation of $CD8^+$ T cells and NK cells (Fig. 6C). When the number of $CD8^+$ T cells was evaluated, no significant differences between WT mice and IFN-γ KO mice were observed (Fig. 6C), which implied that IFN-γ might have no effect on survival and proliferation of $CD8^+$ T cells in this model. The previously observed increase in macrophages was also dependent on IFN-γ (Fig. 6D), but no impairment of DC priming was detected in IFN-γ KO mice (data not shown). In addition to its immuno-regulatory roles, we also found that IFN-γ could directly enhance inhibition of tumor cell growth by AZD8055 *in vitro* (Supplementary Fig. S4).

Discussion

Inhibitors of the mTOR pathway have been used individually and in combination with a variety of cancer therapeutic agents, including chemotherapy, IGF-IR Inhibitors, and trastuzumab (32–34). Our report outlines an innovative immunotherapeutic approach combining a novel ATP-competitive mTOR inhibitor with an agonist αCD40 antibody in an experimental model of metastatic renal cell carcinoma. We demonstrated that combining the mTORC1/mTORC2 inhibitor, AZD8055, with αCD40 induced significant infiltration, proliferation and activation of $CD8^+$ T cells and NK cells in the liver. Th1 cytokines and related chemokines were also significantly elevated by the combination treatment over levels achieved by either agent alone. In addition, the frequency of activated macrophages and DCs in tumor foci was substantially increased following AZD8055/αCD40 treatment, which facilitated a transition of the tumor microenvironment from predominantly immunosuppressive to one that is strongly Th1 in composition.

Recently, the use of the rapamycin analog, temsirolimus, to inhibit mTORC1, in combination with cancer vaccine therapy also showed enhanced anti-tumor responses (35). However, temsirolimus was not able to regulate innate immune cells as we have observed using AZD8055. Furthermore, we show that the mTORC1 inhibitor, rapamycin, was able to modestly inhibit tumor growth to a similar extent as did AZD8055 alone, but unlike AZD8055 it was unable to synergize with αCD40 for enhanced induction of immunomodulatory responses. Although the efficacy of AZD8055 as a single agent was similar to that of rapamycin alone, it remains unclear whether this is due to the suboptimal concentrations of the inhibitors used in our study or whether there are differences with respect to efficacious dose range with mTORC1/2 versus mTORC1 inhibitors. Nevertheless,

our data makes clear that the distinctive benefits of AZD8055 when used in combination with αCD40 cannot be simply attributed to quantitatively increased antigen release by AZD8055-induced tumor destruction that could simply contribute to further maturation of αCD40-primed APC and promotion of subsequent Th1 anti-tumor responses. Instead, when compared with rapamycin, the ATP-competitive mTOR inhibitor more dramatically inhibited protein synthesis and induced G1 cell cycle arrest in several cancer cell lines not only by targeting both mTORC1 and mTORC2 equally, but also by more completely inhibiting 4E-BP1 phosphorylation, which causes more profound inhibition of mTORC1 (8, 9, 36, 37). These different effects on tumor cells or endothelial cells of AZD8055 may result in qualitatively different tumor-derived products, including distinct cytokine and chemokines, which could therefore contribute indirectly to differences in immune cell recruitment and activation. Another possible explanation for the increase of DCs and macrophages induced by AZD8055 but not rapamycin in the liver is that 4E-BP1 dephosphorylation caused by AZD8055 may contribute to the myeloid differentiation program, and thereby alter some biological functions of subsets of mononuclear phagocytes (38). Moreover, we found IFN-γ played important roles in the combination therapy through both directly mediating anti-tumor response and indirectly regulating immune cell survival and functions. The induction of key IFN-γ-inducible proteins ISG15 (interferon-stimulated gene 15) and CXCL10 that mediate IFN responses are enhanced in 4E-BP1(−/−) mouse epithelial fibroblasts, suggesting that AZD8055 inhibition on 4E-BP1 activity may exhibit important regulatory effects in the generation of IFN responses (39). Recently, divergent effects of rapamycin vs. ATP-competitive mTOR inhibitors have been described for tumor cells (6). Our studies underscore the need for additional investigation as to the different roles these agents play in immune system modulation, particularly within certain tumor microenvironments, which may inform new approaches to the use of these agents for treatment of cancer or autoimmune diseases, or for transplantation.

Recent studies documented several promising features of mTOR inhibition that may enhance anti-tumor immunity (10). First, mTOR inhibition can promote IL-12 production by DCs in the presence of LPS (16). Using intracellular staining, we observed only a slight enhancement of LPS-induced IL-12 production by macrophages and DCs from AZD8055-treated mice. Thus, our data are more consistent with a mechanism whereby the increased level of IL-12 in the combination treatment group is mainly due to an overall increase in the number of IL-12-producing macrophages and DCs present in the liver. Second, mTOR inhibition enhances antigen presentation through induction of autophagy (17). Consistently, we also found up-regulation of CD86 and MHC II expression and presentation of tumor-derived GFP protein in DCs and macrophages in AZD8055/αCD40-treated mice, which would be expected to contribute to more effective T cell-mediated responses. The upregulation of NKG2D expression on $CD8^+$ T cells and NK cells by AZD8055/αCD40 treatment may also contribute to their cytotoxic activity against tumors (40, 41). Rapamycin has also been reported to promote $CD8^+$ memory T cell differentiation (42). However, we found that most $CD8^+$ T cells induced by AZD8055/αCD40 in our model were $CD8^+$ effector T cells ($CD44^{high}$, $CD62L^{low}$, data not shown). On the other hand, although mTOR inhibitors are generally considered to have an overall immunosuppressive effect (13, 43, 44), we observed no significant reduction in the number of immune cells (Fig 2B), the activation or proliferation of CD8 and NK cells (Fig 3) as well as the expression of maturation markers by DCs (Fig 4), when results from AZD8055 or rapamycin alone were compared to the vehicle control group. We also observed an increased number of Tregs in the livers of AZD8055/αCD40-treated mice (Supplementary Fig. S5), that is consistent with the earlier observation that mTOR inhibition can promote Treg differentiation (45). Despite the presence of Treg cells, enhanced proliferation and activation of $CD8^+$ T cells and NK cells was observed following combination treatment. Therefore, we conclude that the

immunosuppressive effects of mTOR inhibitors are not dominant in the setting of their combination with powerful immunotherapeutic stimulants such as αCD40.

Although systemic administration of agonist αCD40 has been used in cancer patients to boost $CD8^+$ T cell or NK cell responses to tumors and to break peripheral self-tolerance (21, 46), there is also evidence that it can induce immune suppression in some settings of tumor growth or virus infection (47, 48). We did detect transient infiltration of $CD8^+$ T cells, NK cells and macrophages into liver during the early stage of single agent αCD40 treatment, and long term treatment accelerated the deletion of all these anti-tumor immune cells (data not shown). We propose that persisting functions of $CD8^+$ T cells restored in the AZD8055/αCD40 treatment group result from the enhanced priming by an increased frequency of antigen presenting cells acquiring antigens derived from AZD8055-triggered tumor destruction, and activated by pro-inflammatory cytokines elevated by the combination treatment (47). The mechanism by which AZD8055 administration prevents the loss of macrophages *in vivo* induced by long term αCD40 treatment still needs further investigation. In addition, possible pro-angiogenic effects may result in some settings following CD40 engagement which could be perceived as a limitation of αCD40 for cancer therapy (49). However, we found AZD8055/αCD40 had an overall anti-angiogenic effect (data not shown), which could also contribute to an overall anti-tumor and anti-metastatic effect. One of our previous studies showed that direct ligation of CD40 on Renca tumor cells triggered cytokine production, leukocyte recruitment, and antitumor responses which could be independent of host CD40 expression (24). In the present study, we used Renca-bearing CD40 KO mice to show that Renca-associated CD40 expression was not sufficient for the anti-tumor effects of this combination therapy (Supplementary Fig. S2). Furthermore, we also observed significant expansion of the immune system using the CD40 negative B16 tumor cell line, which further suggests that tumor-derived CD40 expression is not sufficient for immune responses induced by αCD40-based therapy. However, since the antitumor effects of AZD8055/αCD40 were also lost in the B16 tumor model, (Supplementary Fig. S3B), we can not exclude the possibility that CD40 ligation by tumor cells contributes to enhanced immune sensitivity of some tumors. Future studies should be aimed at addressing the striking sensitivity that RCC appears to have for the combined effects of mTOR and CD40 targeted agents. Ongoing studies will also explore the sensitivities of other tumor models towards mTOR and/or CD40-based combination therapies.

In conclusion, our study demonstrates that combining the ATP-competitive mTOR inhibitor AZD8055 with αCD40 induced strongly enhanced Th1 anti-tumor responses through the recruitment and activation of macrophages and DCs in the tumor microenvironment. These events were critical for the overall enhanced anti-tumor effects of this novel combination since depletion of macrophages substantially reduced the overall anti-tumor effects. Overall, these results demonstrate novel immune-stimulating effects that contribute to enhanced anti-tumor activity, suggesting this combination may also distinctively re-structure the tumor microenvironment of RCC in a manner that favors tumor regression.

Supplementary Material

Refer to Web version on PubMed Central for supplementary material.

Acknowledgments

We thank Anjan Thakurta (formerly of AstraZeneca) for helpful discussions. This project was funded in whole or part by the Intramural Research Program of NIH/NCI.

References

1. Hay N, Sonenberg N. Upstream and downstream of mTOR. Genes Dev. 2004; 18:1926–1945. [PubMed: 15314020]
2. McDonald PC, Oloumi A, Mills J, et al. Rictor and integrin-linked kinase interact and regulate Akt phosphorylation and cancer cell survival. Cancer Res. 2008; 68:1618–1624. [PubMed: 18339839]
3. Zhou H, Huang S. The complexes of mammalian target of rapamycin. Curr Protein Pept Sci. 2010; 11:409–424. [PubMed: 20491627]
4. Rini BI, Michaelson MD, Rosenberg JE, et al. Antitumor activity and biomarker analysis of sunitinib in patients with bevacizumab-refractory metastatic renal cell carcinoma. J Clin Oncol. 2008; 26:3743–3748. [PubMed: 18669461]
5. Ellis LM, Hicklin DJ. Pathways mediating resistance to vascular endothelial growth factor-targeted therapy. Clin Cancer Res. 2008; 14:6371–6375. [PubMed: 18927275]
6. Sparks CA, Guertin DA. Targeting mTOR: prospects for mTOR complex 2 inhibitors in cancer therapy. Oncogene. 2010; 29:3733–3744. [PubMed: 20418915]
7. Shor B, Gibbons JJ, Abraham RT, Yu K. Targeting mTOR globally in cancer: thinking beyond rapamycin. Cell Cycle. 2009; 8:3831–3837. [PubMed: 19901542]
8. Feldman ME, Apsel B, Uotila A, et al. Active-site inhibitors of mTOR target rapamycin-resistant outputs of mTORC1 and mTORC2. PLoS Biol. 2009; 7:e38. [PubMed: 19209957]
9. Thoreen CC, Kang SA, Chang JW, et al. An ATP-competitive mammalian target of rapamycin inhibitor reveals rapamycin-resistant functions of mTORC1. J Biol Chem. 2009; 284:8023–8032. [PubMed: 19150980]
10. Thomson AW, Turnquist HR, Raimondi G. Immunoregulatory functions of mTOR inhibition. Nat Rev Immunol. 2009; 9:324–337. [PubMed: 19390566]
11. Saunders RN, Metcalfe MS, Nicholson ML. Rapamycin in transplantation: a review of the evidence. Kidney Int. 2001; 59:3–16. [PubMed: 11135052]
12. Wai LE, Fujiki M, Takeda S, Martinez OM, Krams SM. Rapamycin, but not cyclosporine or FK506, alters natural killer cell function. Transplantation. 2008; 85:145–149. [PubMed: 18192925]
13. Hackstein H, Taner T, Zahorchak AF, et al. Rapamycin inhibits IL-4--induced dendritic cell maturation in vitro and dendritic cell mobilization and function in vivo. Blood. 2003; 101:4457–4463. [PubMed: 12531798]
14. Fox R, Nhan TQ, Law GL, Morris DR, Liles WC, Schwartz SM. PSGL-1 and mTOR regulate translation of ROCK-1 and physiological functions of macrophages. EMBO J. 2007; 26:505–515. [PubMed: 17245434]
15. Weinstein SL, Finn AJ, Dave SH, et al. Phosphatidylinositol 3-kinase and mTOR mediate lipopolysaccharide-stimulated nitric oxide production in macrophages via interferon-beta. J Leukoc Biol. 2000; 67:405–414. [PubMed: 10733102]
16. Weichhart T, Costantino G, Poglitsch M, et al. The TSC-mTOR signaling pathway regulates the innate inflammatory response. Immunity. 2008; 29:565–577. [PubMed: 18848473]
17. Jagannath C, Lindsey DR, Dhandayuthapani S, Xu Y, Hunter RL Jr, Eissa NT. Autophagy enhances the efficacy of BCG vaccine by increasing peptide presentation in mouse dendritic cells. Nat Med. 2009; 15:267–276. [PubMed: 19252503]
18. Grewal IS, Flavell RA. CD40 and CD154 in cell-mediated immunity. Annu Rev Immunol. 1998; 16:111–135. [PubMed: 9597126]
19. Ridge JP, Di Rosa F, Matzinger P. A conditioned dendritic cell can be a temporal bridge between a CD4+ T-helper and a T-killer cell. Nature. 1998; 393:474–478. [PubMed: 9624003]
20. French RR, Taraban VY, Crowther GR, et al. Eradication of lymphoma by CD8 T cells following anti-CD40 monoclonal antibody therapy is critically dependent on CD27 costimulation. Blood. 2007; 109:4810–4815. [PubMed: 17311995]
21. Turner JG, Rakhmilevich AL, Burdelya L, et al. Anti-CD40 antibody induces antitumor and antimetastatic effects: the role of NK cells. J Immunol. 2001; 166:89–94. [PubMed: 11123280]

22. Hayashi T, Treon SP, Hideshima T, et al. Recombinant humanized anti-CD40 monoclonal antibody triggers autologous antibody-dependent cell-mediated cytotoxicity against multiple myeloma cells. Br J Haematol. 2003; 121:592–596. [PubMed: 12752100]
23. Vonderheide RH, Flaherty KT, Khalil M, et al. Clinical activity and immune modulation in cancer patients treated with CP-870,893, a novel CD40 agonist monoclonal antibody. J Clin Oncol. 2007; 25:876–883. [PubMed: 17327609]
24. Shorts L, Weiss JM, Lee JK, et al. Stimulation through CD40 on mouse and human renal cell carcinomas triggers cytokine production, leukocyte recruitment, and antitumor responses that can be independent of host CD40 expression. J Immunol. 2006; 176:6543–6552. [PubMed: 16709811]
25. Williams PD, Pontes EJ, Murphy GP. Studies of the growth of a murine renal cell carcinoma and its metastatic patterns. Res Commun Chem Pathol Pharmacol. 1981; 34:345–349. [PubMed: 7335958]
26. Gruys ME, Back TC, Subleski J, et al. Induction of transplantable mouse renal cell cancers by streptozotocin: in vivo growth, metastases, and angiogenic phenotype. Cancer Res. 2001; 61:6255–6263. [PubMed: 11507080]
27. Fogler WE, Volker K, Watanabe M, et al. Recruitment of hepatic NK cells by IL-12 is dependent on IFN-gamma and VCAM-1 and is rapidly down-regulated by a mechanism involving T cells and expression of Fas. J Immunol. 1998; 161:6014–6021. [PubMed: 9834083]
28. Livak KJ, Schmittgen TD. Analysis of relative gene expression data using real-time quantitative PCR and the 2(-Delta Delta C(T)) Method. Methods. 2001; 25:402–408. [PubMed: 11846609]
29. Sini P, James D, Chresta C, Guichard S. Simultaneous inhibition of mTORC1 and mTORC2 by mTOR kinase inhibitor AZD8055 induces autophagy and cell death in cancer cells. Autophagy. 2010:6.
30. Chresta CM, Davies BR, Hickson I, et al. AZD8055 is a potent, selective, and orally bioavailable ATP-competitive mammalian target of rapamycin kinase inhibitor with in vitro and in vivo antitumor activity. Cancer Res. 2010; 70:288–298. [PubMed: 20028854]
31. Subleski JJ, Hall VL, Back TC, Ortaldo JR, Wiltrout RH. Enhanced antitumor response by divergent modulation of natural killer and natural killer T cells in the liver. Cancer Res. 2006; 66:11005–11012. [PubMed: 17108139]
32. Mondesire WH, Jian W, Zhang H, et al. Targeting mammalian target of rapamycin synergistically enhances chemotherapy-induced cytotoxicity in breast cancer cells. Clin Cancer Res. 2004; 10:7031–7042. [PubMed: 15501983]
33. Geoerger B, Kerr K, Tang CB, et al. Antitumor activity of the rapamycin analog CCI-779 in human primitive neuroectodermal tumor/medulloblastoma models as single agent and in combination chemotherapy. Cancer Res. 2001; 61:1527–1532. [PubMed: 11245461]
34. Wan X, Harkavy B, Shen N, Grohar P, Helman LJ. Rapamycin induces feedback activation of Akt signaling through an IGF-1R-dependent mechanism. Oncogene. 2007; 26:1932–1940. [PubMed: 17001314]
35. Wang Y, Wang XY, Subjeck JR, Shrikant PA, Kim HL. Temsirolimus, an mTOR inhibitor, enhances anti-tumour effects of heat shock protein cancer vaccines. Br J Cancer. 2011; 104:643–652. [PubMed: 21285988]
36. Shor B, Zhang WG, Toral-Barza L, et al. A new pharmacologic action of CCI-779 involves FKBP12-independent inhibition of mTOR kinase activity and profound repression of global protein synthesis. Cancer Res. 2008; 68:2934–2943. [PubMed: 18413763]
37. Yu K, Toral-Barza L, Shi C, et al. Biochemical, cellular, and in vivo activity of novel ATP-competitive and selective inhibitors of the mammalian target of rapamycin. Cancer Res. 2009; 69:6232–6240. [PubMed: 19584280]
38. Grolleau A, Sonenberg N, Wietzerbin J, Beretta L. Differential regulation of 4E-BP1 and 4E-BP2, two repressors of translation initiation, during human myeloid cell differentiation. J Immunol. 1999; 162:3491–3497. [PubMed: 10092805]
39. Kaur S, Lal L, Sassano A, et al. Regulatory effects of mammalian target of rapamycin-activated pathways in type I and II interferon signaling. J Biol Chem. 2007; 282:1757–1768. [PubMed: 17114181]

40. Walsh KB, Lanier LL, Lane TE. NKG2D receptor signaling enhances cytolytic activity by virus-specific CD8+ T cells: evidence for a protective role in virus-induced encephalitis. J Virol. 2008; 82:3031–3044. [PubMed: 18160433]
41. Westwood JA, Kelly JM, Tanner JE, Kershaw MH, Smyth MJ, Hayakawa Y. Cutting edge: novel priming of tumor-specific immunity by NKG2D-triggered NK cell-mediated tumor rejection and Th1-independent CD4+ T cell pathway. J Immunol. 2004; 172:757–761. [PubMed: 14707044]
42. Rao RR, Li Q, Odunsi K, Shrikant PA. The mTOR kinase determines effector versus memory CD8+ T cell fate by regulating the expression of transcription factors T-bet and Eomesodermin. Immunity. 2010; 32:67–78. [PubMed: 20060330]
43. Yang Q, Guan KL. Expanding mTOR signaling. Cell Res. 2007; 17:666–681. [PubMed: 17680028]
44. Woltman AM, de Fijter JW, Kamerling SW, et al. Rapamycin induces apoptosis in monocyte- and CD34-derived dendritic cells but not in monocytes and macrophages. Blood. 2001; 98:174–180. [PubMed: 11418477]
45. Delgoffe GM, Kole TP, Zheng Y, et al. The mTOR kinase differentially regulates effector and regulatory T cell lineage commitment. Immunity. 2009; 30:832–844. [PubMed: 19538929]
46. Vonderheide RH. Prospect of targeting the CD40 pathway for cancer therapy. Clin Cancer Res. 2007; 13:1083–1088. [PubMed: 17317815]
47. Kedl RM, Jordan M, Potter T, Kappler J, Marrack P, Dow S. CD40 stimulation accelerates deletion of tumor-specific CD8(+) T cells in the absence of tumor-antigen vaccination. Proc Natl Acad Sci U S A. 2001; 98:10811–10816. [PubMed: 11526222]
48. Bartholdy C, Kauffmann SO, Christensen JP, Thomsen AR. Agonistic anti-CD40 antibody profoundly suppresses the immune response to infection with lymphocytic choriomeningitis virus. J Immunol. 2007; 178:1662–1670. [PubMed: 17237416]
49. Murugaiyan G, Martin S, Saha B. CD40-induced countercurrent conduits for tumor escape or elimination? Trends Immunol. 2007; 28:467–473. [PubMed: 17981086]

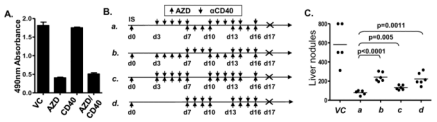

Figure 1.

AZD8055 plus αCD40 inhibited Renca tumor development in liver. A, *In vitro* MTS proliferation assay for Renca cells. Renca cells were stimulated with αCD40 (100ug/ml), AZD8055 (AZD) (50ng/ml) or both for 72 hours. For the *in vivo* tumor model study, Renca cells were injected intrasplenically. Splenectomies were done on all mice immediately after tumor injection. αCD40 (65 ug, i.p.) and AZD8055 (20mg/kg weight, oral gavage) were administered on the indicated days as shown in (B). C, All mice were then euthanized on day 17, and liver tumor nodules were counted. All data are representative of two or three independent experiments.

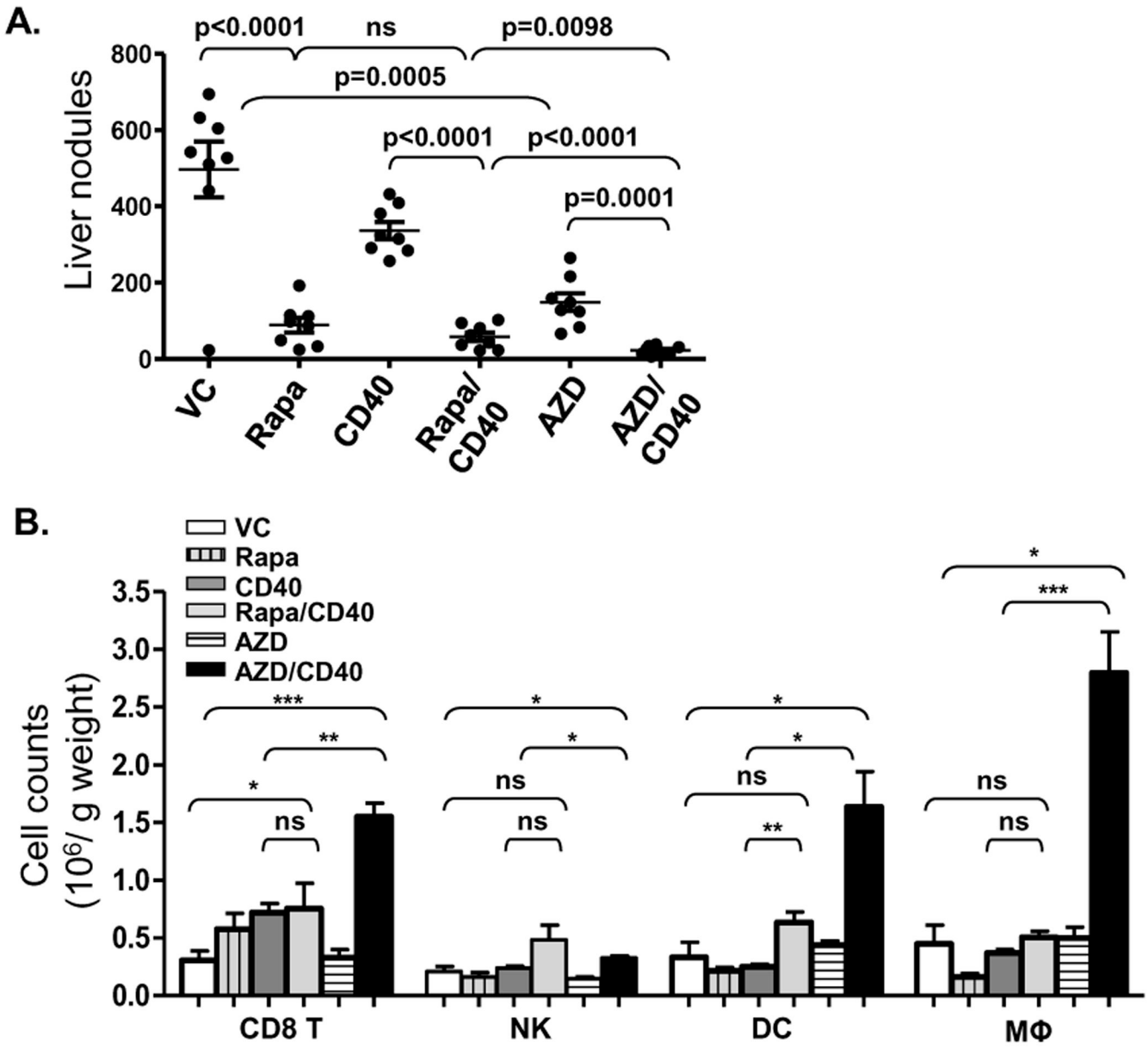

Figure 2.

AZD8055, but not rapamycin enhanced αCD40 -induced anti-tumor immune responses. A, Renca cells were injected intrasplenically. Splenectomies were done on all mice immediately after tumor injection. αCD40 (65 ug, i.p.), rapamycin (Rapa) (2 mg/kg weight, oral gavage), and AZD8055 (20mg/kg weight, oral gavage) were administered according to schedule *a* in Fig. 1B. Mice were euthanized on day 17 and liver tumor nodules counted. B, Hepatic mononuclear cells were isolated from livers on day 14 and analyzed through flow cytometry. $CD8^+$ T cells, NK cells, DCs and macrophages were identified as $CD3^+CD8^+CD45^+$ cells and $CD3^-NKp46^+CD45^+$ cells, $CD3^-NKp46^-F4/80^-CD11c^+$ $CD45^+$ cells and $F4/80^+CD45^+$ cells, respectively. All data are representative of two or three independent experiments. *, $p<0.05$, ** $p<0.01$, *** $p<0.001$.

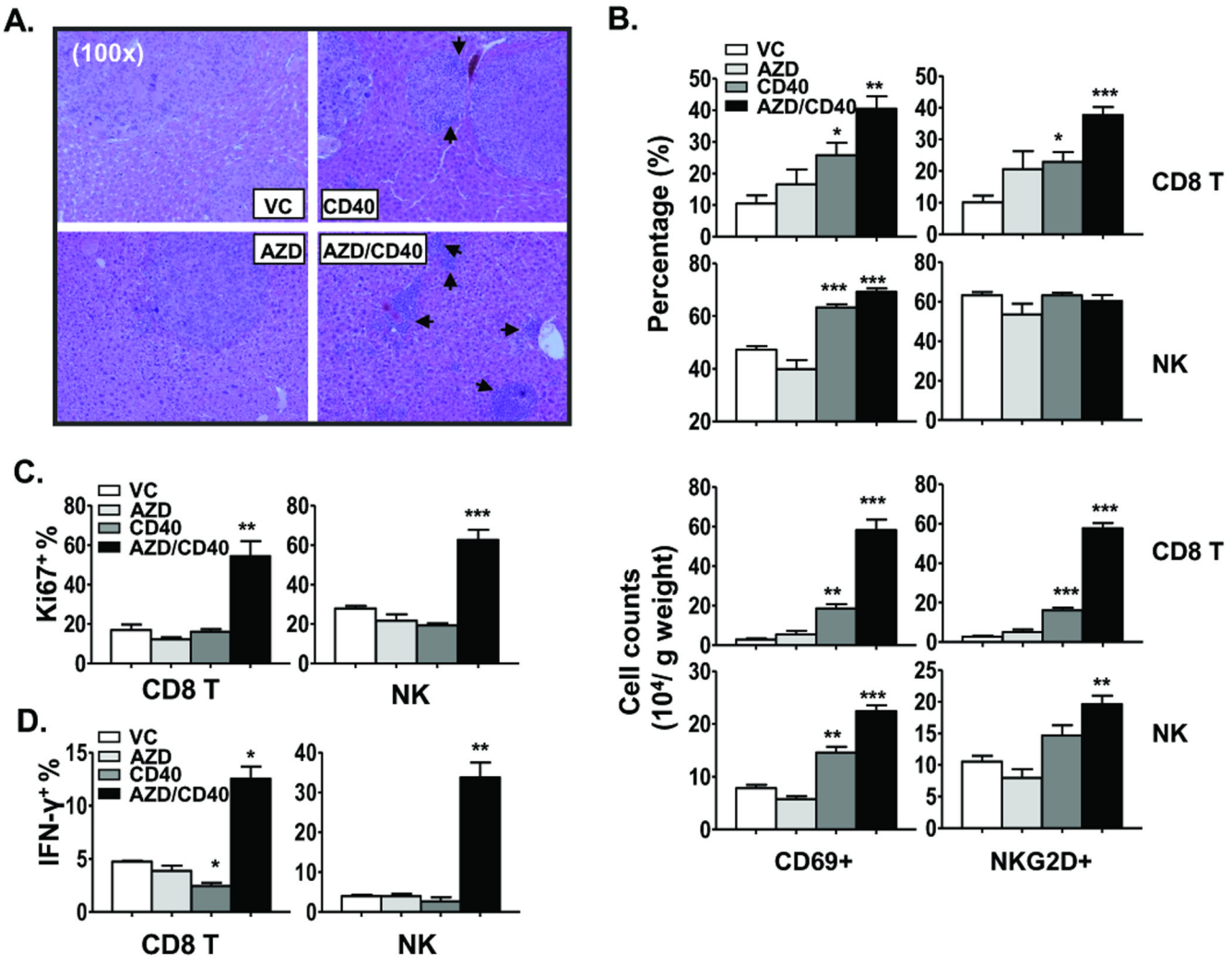

Figure 3.

AZD8055/αCD40 induced activation of CD8 T cells and NK cells *in vivo*. Renca cells were injected intrasplenically. Splenectomies were done on all mice immediately after tumor injection αCD40 (65 ug, i,.p.) and AZD8055 (20mg/kg weight, oral gavage) were administered according to schedule *a* in Figure 1B. A, Hematoxylin and eosin staining of liver tissue on day 17. Arrows point to lymphocyte infiltration. B, Hepatic mononuclear cells were isolated from livers on day 14 and analyzed by flow cytometry. Percentages of $CD69^+$ and $NKG2D^+$ cells among $CD8^+$ T cells and NK cells were shown, as well as the absolute number. C–D, Hepatic mononuclear cells were isolated on day 17. Ki67 expression and IFN-γ production by $CD8^+$ T cells and NK cells were analyzed by flow cytometry with intracellular staining. Percentages of $Ki67^+$ (C) and IFN-γ^+ cells (D) among $CD8^+$ T cells and NK cells are shown. *, $p<0.05$, ** $p<0.01$, *** $p<0.001$, VC control group versus all other groups. D, All data are representative of two or three independent experiments.

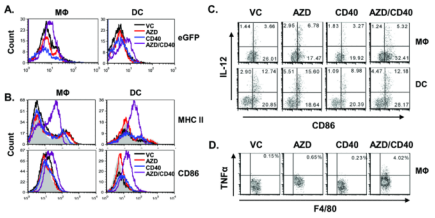

Figure 4.

Macrophages and DCs were activated in livers of AZD8055/αCD40 -treated mice. eGFP-expressing Renca (A) or Renca cells (B–D) were injected intrasplenically. Splenectomies were done on all mice immediately after tumor injection αCD40 (65 μg, i,.p.) and AZD8055 (20mg/kg weight, oral gavage) were administered according to schedule *a* in Figure 1B. Hepatic mononuclear cells were isolated from livers on day 14 and analyzed by flow cytometry. Macrophages and DCs were identified as $F4/80^{+}CD45^{+}$ cells and $CD3^{-}NKp46^{-}F4/80^{-}CD11c^{+}$ $CD45^{+}$ cells, respectively. A, eGFP phagocytosis by macrophages and DCs, B, CD86 and MHC class II expression on macrophages and DCs. The gray solid area in the histogram represents isotype control staining. C–D, IL-12 production by macrophages and DCs (C) and TNFα production by macrophages (D) were evaluated by intracellular staining, with LPS restimulation performed as indicated in the *Materials and Methods* section. Numbers indicate the percentages among macrophages or DCs. All data are representative of two or three independent experiments.

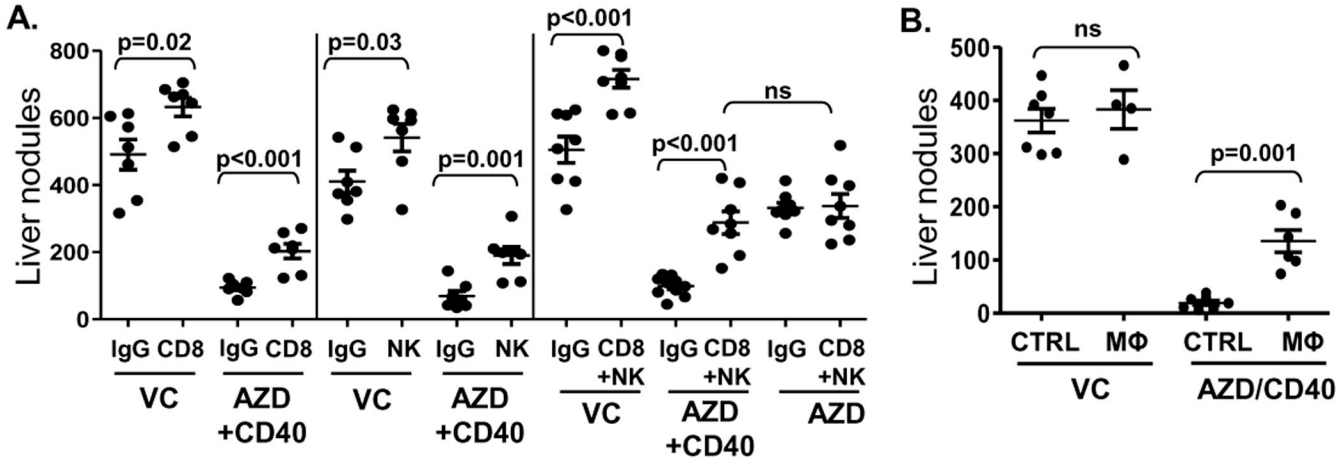

Figure 5.

A, $CD8^+$ T cell depletion treatment was initiated on day 3 and performed twice a week. NK cell depletion treatment was initiated 24 hours before Renca implantation and repeated on days 2, 4, 6 and 13 using anti-asGM1 antibody. B, Macrophages were depleted using i.v. injection of clodronate liposomes on day -1, 2, 6, 10, 14. PBS-containing liposomes were used as a control. Liver tumor nodules were counted on day 17.

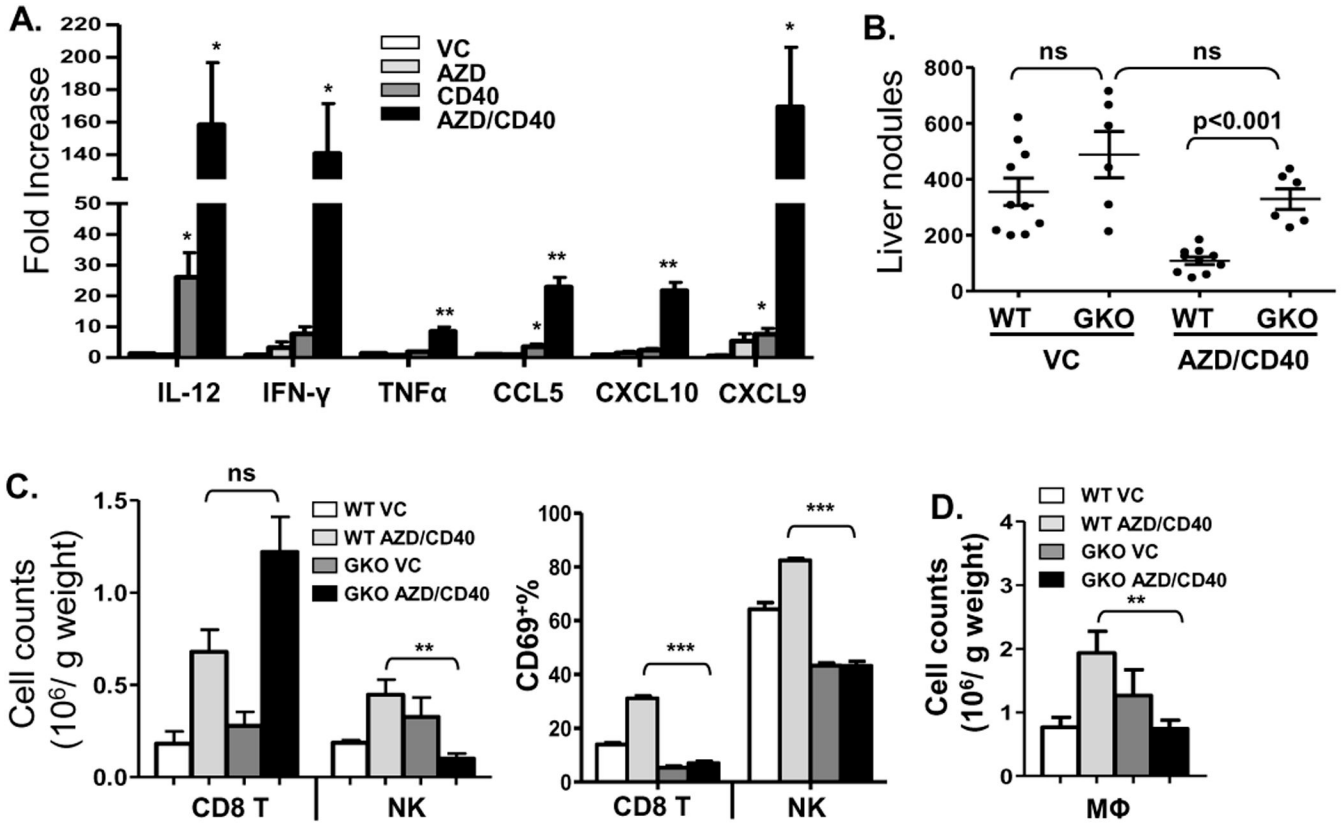

Figure 6.

AZD8055/αCD40 induced anti-tumor responses were dependent on IFN-γ. A, Real-time quantitative PCR was used to analyze IL-12, IFN-γ, TNFα, CCL5, CXCL10, and CXCL9 expression in the livers of AZD8055/αCD40 treated tumor-bearing mice on day 17. * $p<0.05$, ** $p<0.01$, VC control group versus all other groups. B, Anti-tumor responses induced by AZD8055/αCD40 were evaluated in IFN-γ KO (GKO) mice. Liver nodules were counted on day 17. C–D, Hepatic MNCs were isolated from IFN-γ KO mice on day 14 and analyzed by flow cytometry. Absolute numbers of $CD8^+$ T cells and NK cells and percentage of $CD69^+$ cells among them in IFN-γ KO mice are shown in (C). Absolute number of macrophages was shown in (D). * $p<0.05$, ** $p<0.01$, *** $p<0.001$. All data are representative of two or three independent experiments.